Reversible Micelle−Vesicle Conversion of Oleyldimethylamine Oxide by pH Changes

Hiroshi Maeda,*,† Shimon Tanaka,† Yousuke Ono,† Masahiko Miyahara,† Hideya Kawasaki,† Norio Nemoto,‡ and Mats Almgren§

Department of Chemistry, Faculty of Sciences, Kyushu University, Fukuoka 812-8581, Japan, Department of Molecular and Material Sciences, IGSES, Kyushu University, Fukuoka 812-8581, Japan, and Department of Physical Chemistry, Box 579, Uppsala University, S 751-23, Uppsala, Sweden

Received: November 30, 2005; In Final Form: May 5, 2006

A preliminary study on the reversible micelle−vesicle conversion of oleyldimethylamine oxide [Kawasaki, H. et al. *J. Phys. Chem. B.* **2002**, 106, 1524] is extended in the present study. In the presence of 0.01 M NaCl at a surfactant concentration of 0.05 M, a micelle-to-vesicle conversion with increasing degree of ionization α takes place in the following sequence: growth of fibrous micelle ($\alpha < 0.2$), a fused network ($\alpha \sim 0.3$), fibrous micelles + (perforated) vesicles ($\alpha = 0.4$), and vesicles + lamellae ($\alpha = 0.5$). Viscoelasticity correspondingly varies from the Maxwell-type behavior of the entangled network of fibrous micelles to the gel-like behavior of vesicle suspensions, via a fluid solution-like behavior of the fused network. This phase sequence is in contrast with the case of no added salt where no branching of micelles is observed, and long micelles and bilayers (vesicles + lamellae) coexist at $\alpha = 0.5$. In water, a state of the lowest viscoelasticity occurs around $\alpha = 0.2$ for both surfactant concentrations 0.05 and 0.15 M. Synergism between protonated and nonprotonated amine oxide headgroups is observed despite low ionic strengths. From the time course of the reversible micelle−vesicle conversion, vesicles seem to be formed from threadlike micelles within 25 h according to the shear moduli, while a longer conversion time is suggested by a flow property (viscosity). Shear thickening behavior is observed at $\alpha = 0.2$ and 0.4 in 0.01 M NaCl but not in water.

Introduction

Surfactants can form various self-assemblies in dilute aqueous solutions including micelles, vesicles, and bilayers. These structures are useful in various applications such as encapsulation of drugs or other substances, solubilization of water-insoluble material in aqueous media, and for chemical reactions in a confined space. In recent years, various systems including single-chain amphiphiles have been reported to form vesicles and these results are summarized in review articles.[1−6]

Theoretical descriptions of the vesicle formation have been developed in both elastic continuum approaches[7,8] and molecular approaches.[9−11] A combined approach has been recently reported.[12] According to Helfrich,[7] the elastic energy per unit area of a bilayer E_b is written in terms of the binding constant k_b and the saddle-splay constant k_G.

$$E_b = (k_b/2)(H_1 + H_2 - 2H_0)^2 + k_b H_1 H_2 \qquad (k_b > 0) \quad (1)$$

Here H_1, H_2, and H_0 denote the two principal curvatures and the spontaneous curvature. For a spherical vesicle of radius R, $H_1 = H_2 = H = 1/R$ and eq 1 reduces to eq 2.

$$E_b = 2k_b(H - H_0)^2 + k_G H^2 \quad (2)$$

For symmetric bilayers, $H_0 = 0$ and $E_b = (2k_b + k_G)H^2$. Since $(2k_b + k_G)$ is generally positive, vesicles of symmetric bilayers are not stable with respect to the energy and vesicle solutions are often only kinetically stable. If the $(2k_b + k_G)$ value is small and positive, the translational and mixing entropy associated with dispersed particles could overcome the energy penalty, and vesicles may become thermodynamically stable. For charged bilayers, it has been suggested that k_G becomes negative[8,13−15] and hence for soft bilayers ($k_b \sim kT$), E_b could be negative. For multicomponent vesicles, bilayers can be asymmetric and H_0 is non-zero if the compositions differ for the outer and the inner layers. At $H = H_0$, then E_b is $k_G H^2$ that is either small positive or even negative.

A reasonable classification of vesicles consisting of single chain amphiphiles has been proposed by Lasic et al.,[3] on the basis of the number of components constituting the vesicle. Among several classes, there is one characterized by two-component mixtures. Vesicles formed by fatty acids and their soaps (acid soaps) belong to this category.[16−19] As a result of the complex formation through the hydrogen bond between carboxyl and the carboxylate headgroup, they behave like double chain amphiphiles which prefer structures of small curvatures. Amine oxides have been shown to be capable of forming a similar kind of complex through hydrogen bonding between protonated (−NOH) and nonprotonated (−NO) amine oxide groups.[20−22] Among other examples are alcohol/SDS mixtures[23] and mixtures of zwitterionic and ionic amphiphiles.[24] Catanionic vesicles may also belong to this class.[25−29] Kaler and collaborators reported on spontaneous vesicle formation by an unbalanced mixing of cationic and anionic surfactants, resulting in finite curvatures of bilayers due to electric repulsion.

To understand the underlying fundamental principles of spontaneous vesiculation, it is useful to develop reversible micelle−vesicle conversions by changing a physical parameter

* Address correspondence to this author. Phone: +81-92-681-8080. Fax: +81-92-642-2607. E-mail: h.maescc@mbox.nc.kyushu-u.ac.jp.
† Faculty of Science, Kyushu University.
‡ Department of Molecular and Material Sciences, IGSES, Kyushu University.
§ Department of Physical Chemistry, Uppsala University.

10.1021/jp056967c CCC: $33.50
Published on Web 06/03/2006

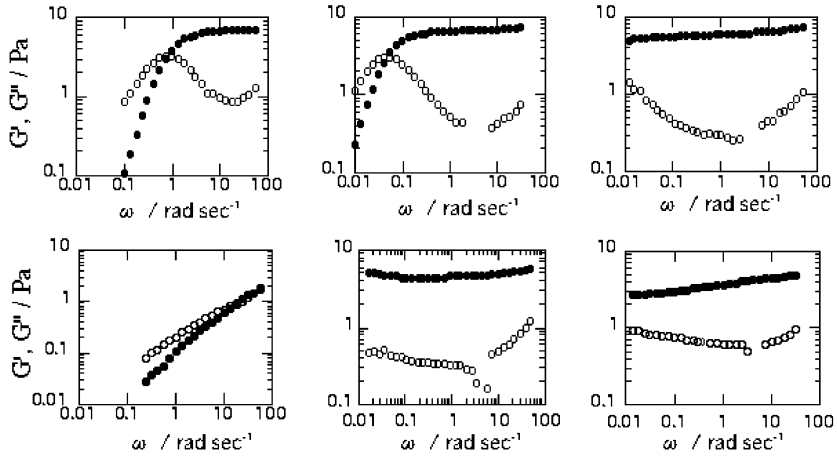

Figure 1. Angular frequency ω dependence of the storage shear modulus G' (closed circles) and the loss shear modulus G'' (open circles) of oleylDMAO solutions with different degrees of ionization α at $C = 0.05$ M in 0.01 M NaCl aqueous solutions at 25 °C: (a) $\alpha = 0$, (b) $\alpha = 0.1$, (c) $\alpha = 0.2$, (d) $\alpha = 0.3$, (e) $\alpha = 0.4$, and (f) $\alpha = 0.5$.

such as temperature, pressure, or pH of the medium. There have been a few reports on reversible vesicle−micelle conversion. Temperature-dependent vesicle−micelle conversion has been reported for hexadecyltrimethylammonium chloride−2-hydroxynaphthalene carboxylate.[30,31] Also, temperature-dependent dispersion/aggregation of vesicles was recently reported.[32,33]

In the first report on the reversible micelle−vesicle conversion by changing pH, oleyldimethylamine oxide was shown to form micelles at low degrees of ionization (pH >6), while it formed vesicles at a degree of ionization around 0.5 (pH ∼5).[22] Other pH-sensitive vesicles have been reported.[34,35]

Introduction of electric charges generally increases the average curvature of a monolayer and facilitates the formation of vesicles from the lamella phase, also by strongly swelling the lamellar phase, and by stabilizing the vesicles.[36,37] The change of the average curvature by protonation of alkylamine oxides has been shown to differ from the expectation based on purely electrostatic interaction: the average curvature goes through a minimum at about the half-protonated state.[20,22,38−43] This characteristic behavior has been attributed to a hydrogen bond between the protonated and the nonprotonated headgroups of amine oxide.[20] Spectroscopic information has been obtained in favor of this proposed hydrogen bond.[21]

In the present study, we are going to report on a two-component vesicle, oleyldimethylamine oxide (oleylDMAO)/oleyldimethylhydroxylammonium chloride (oleylDMAOH$^+$Cl$^-$). Effects of the degree of ionization on the aggregate structures in the solution and reversibility of the structural change with respect to pH changes are examined by viscoelasticity and cryoTEM. The mixture forms vesicles at a mixing ratio close to 1:1. The system is also unique in the respect that the micelle−vesicle conversion is reversibly controlled by the pH of the solution. A preliminary report of the present study has been published.[22]

Experimental Section

Oleyldimethyamine oxide was obtained from oleyldimethylamine (Lion Akzo) through the oxidation in ethanol by hydrogen peroxide following, in most part, the similar procedure as for other alkyldimethylamine oxides and purified by the extraction of the unreacted amine by hexane.[22] The surface tension showed no minimum around the critical micelle concentration [$(8 \pm 1) \times 10^{-5}$ mol (kg water)$^{-1}$]. The surfactant concentration C was actually in mol (kg water)$^{-1}$, but for the sake of simple presentation, it is expressed in molarity, M, in this paper assuming the associated errors are insignificant. The viscoelastic properties were measured at 25 ± 0.1 °C with a stress-controlled rheometer (Carri-MED CSL-100) with a cone plate (plate diameter 6 cm, 2° angle) and a parallel plate type geometry (plate diameter 4 cm) on oleylDMAO solutions.

The electron microscopy investigations were performed with a Zeiss 902 A instrument, operating at 80 kV. Specimens were prepared by a blotting procedure, performed in a chamber with controlled temperature and humidity. A drop of the sample solution was placed onto an EM grid coated with a perforated polymer film. Excess solution was then removed with a filter paper, leaving a thin film of the solution on the EM grid. Vitrification of the thin film was achieved by rapid plunging of the grid into liquid ethane held at its freezing point. The vitrified specimen was then transferred in the cold state to the microscope and investigated at 108 K.

Results

1. Effects of the Protonation in 0.01 M NaCl Aqueous Solutions at 25 °C. Figure 1 shows angular frequency ω dependence of the storage shear modulus G' and the loss shear modulus G'' of oleylDMAO solutions with different degrees of ionization α at $C = 0.05$ M. At the degrees of ionization $\alpha = 0$ and 0.1 (Figure 1a,b), the behavior is characteristic of a transient network consisting of long flexible chains that can be described with the Maxwell model.[44−46] The longest relaxation times τ were 1.2 and 20 s for $\alpha = 0$ and 0.1, respectively. A minimum of G'' was observed for $\alpha = 0$, 0.1, and 0.2 with $G''_{min} \sim 0.6-0.7$, 0.2−0.3, and 0.15−0.2 Pa, respectively. With values of G'_N of about 8 and 6.6−6 Pa for $\alpha = 0$ and 0.1−0.2, the ratio G''_{min}/G'_N is about 8×10^{-2} and 4×10^{-2} to 3×10^{-2}, respectively. The decrease of the ratio G''_{min}/G'_N with increasing α is consistent with a picture of micelle growth by protonation.

The viscoelastic behavior of oleylDMAO dramatically changed on further protonation as shown in Figure 1d. At $\alpha = 0.3$, solutions were much more fluidlike than at other α values. At $\alpha = 0.4$ and 0.5, both G' and G'' exhibited very weak dependence on frequency ω and a relation $G' > G''$ was observed suggesting a kind of gel or solid state consisting of densely packed particles (Figure 1e,f). These results resemble those of vesicle suspensions of amine oxide/ionic surfactant mixtures.[47] As α increases from 0.4 to 0.5, G' decreased while G'' increased.

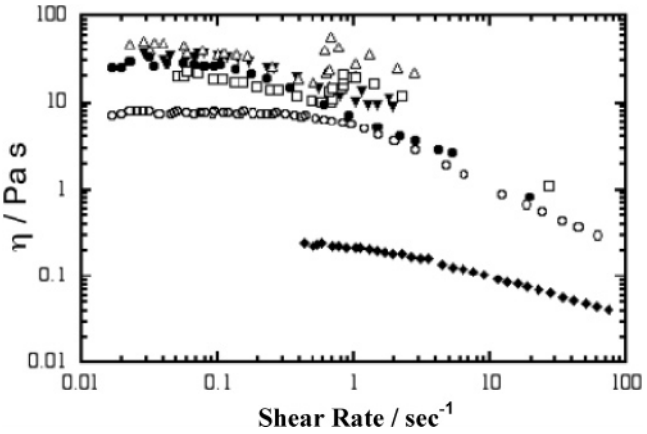

Figure 2. Shear rate dependence of the solution viscosity at different α values at $C = 0.05$ M in 0.01 M NaCl aqueous solutions at 25 °C: α = 0 (open circles), α = 0.1 (filled circles), α = 0.2 (open triangles), α = 0.3 (filled diamonds), α = 0.4 (open squares), and α = 0.5 (inverted filled triangles).

Figure 2 shows the shear rate dependence of the solution viscosity at different α values. At α = 0, shear thinning occurs in the range of the shear rate greater than about 1 s^{-1} with a slope of -0.77 ± 0.03. At α = 0.1, viscosity increases and shear thinning starts at a shear rate around 0.2 s^{-1}. At α = 0.2, the viscosity becomes the largest and shear thinning starts at a shear rate around 0.05 s^{-1}, followed by shear thickening in the range of shear rate around 0.5 s^{-1}. Onset shear rate values for the shear thinning decrease as α increases from 0 to 0.2. The viscosity behavior in the range of α = 0−0.2 is consistent with micelle growth with increasing α as suggested in Figure 1. When zero shear viscosity η_0 is estimated in Figure 2, the relation $\eta_0 = G'_N\tau$ approximately holds at α = 0 and 0.1. At α = 0.2, the solution behavior differs from that of typical Maxwell as shown by a shear thickening behavior and the relation $\eta_0 = G'_N\tau$ does not hold. In contrast to the results at α = 0−0.2, the viscosity is strongly reduced at α = 0.3. At α = 0.4 and 0.5, the viscosity increases to a range of values larger than at α = 0. The viscosity of the two solutions is rather similar at low shear rates but differs in the shear rate range larger than about 1 s^{-1}, with shear thickening for α = 0.4, and shear thinning for α = 0.5. It is to be noted that shear thickening was observed only at α = 0.2 and 0.4. In the solutions without added salt, shear thickening was not observed (Figure 5), although a time-dependent viscosity increase was observed for α = 0.5 under a constant shear rate.[48] Association of rodlike micelles by shear as proposed by Hofmann[49] is a probable mechanism of the shear thickening at α = 0.2, while another mechanism should be responsible for the thickening at α = 0.4, such as a shear-induced conversion from vesicles to long fibrous micelles.[50] Dependence of the viscoelastic properties on α is summarized in Figure 9 together with the results in water and is discussed later.

The drastic changes in the viscoelastic properties shown in Figures 1 and 2 are found to correspond to different aggregate structures as shown in Figure 3, displaying cryo-transmission electron micrographs (cryo-TEM) of the solutions at different degrees of protonation. At α = 0.3, branching of micelles was observed, Figure 3a. The entangled network of long fibrous micelles at α < 0.2 is now transformed into a fused network thereby giving high fluidity to the solution of α = 0.3. The fused network of micelles was proposed by Porte[51,52] and was observed by Danino et al.[53] and others.[24,54,55] The very fluidlike nature of this structure has been reported.[52,56] A negative curvature (concave toward aqueous phase) required to form

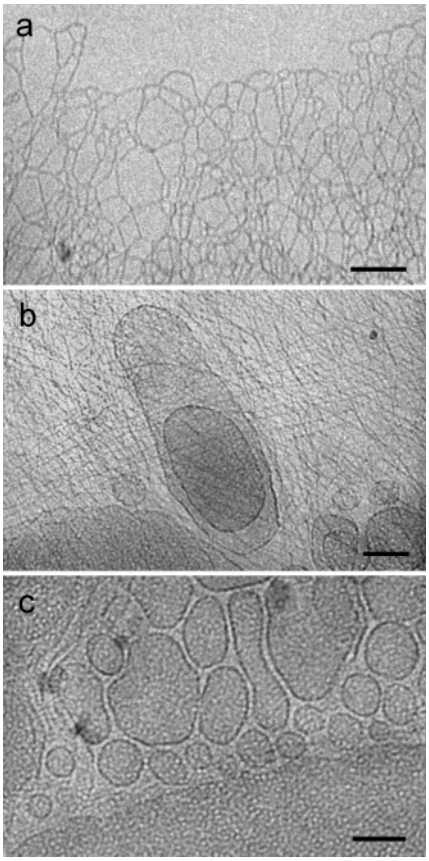

Figure 3. Cryoscopic transmission electron micrographs of oleylDMAO solutions at $C = 0.05$ M in 0.01 M NaCl aqueous solutions. The bar in each figure corresponds to 100 nm: (a) α = 0.3, (b) α = 0.4, and (c) α = 0.5.

branching points is expected to become possible, because the free energy cost associated with the formation is reduced considerably as a result of the increased shielding of electric repulsion in 0.01 M NaCl. At α = 0.4, both long fibrous micelles and vesicles coexist, as shown in Figure 3b. At α = 0.5, closely packed vesicles and lamellae are coexisting and the vesicles are more or less perforated as shown in Figure 3c.

In the present study, the transition from micelles to vesicles follows a sequence characterized by a rather continuous decrease of the average curvature with ionization: growth of fibrous micelles, a fused network, vesicles + fibrous micelles, and finally vesicles + lamellae. The changes in the viscoelastic properties are consistent with the cryoTEM observations.

2. Micelle−Vesicle Conversion in Water at 25 °C and C = 0.15 M. Figure 4 shows angular frequency ω dependence of the storage shear modulus G' and the loss shear modulus G'' of oleylDMAO solutions with different degrees of ionization α at $C = 0.15$ M. At the degrees of ionization α = 0 (nonionic state) and 0.1, behaviors characteristic to an entangled network consisting of long flexible chains are seen. The slowest relaxation times τ were about 1 and 10 s for α = 0 and 0.1. A minimum of G'' was found at α = 0 and 0.1 with $G''_{min} \sim 3$ and 0.7 Pa and $G'_N \sim 50$ and 65 Pa, resulting in the ratio $G''_{min}/G'_N \sim 4.5 \times 10^{-2}$ and 1.3×10^{-2}, respectively. The decrease of the ratio G''_{min}/G'_N with increasing α is consistent with the micelle growth by protonation, as observed in 0.01 M NaCl.

The viscoelastic behavior of oleylDMAO dramatically changed on further protonation. At α = 0.2, solutions were more fluidlike than at α = 0 and 0.1. (The data of Figure 1b of ref 22 corresponds to α = 0.1, though assigned to α = 0.2 by mistake.)

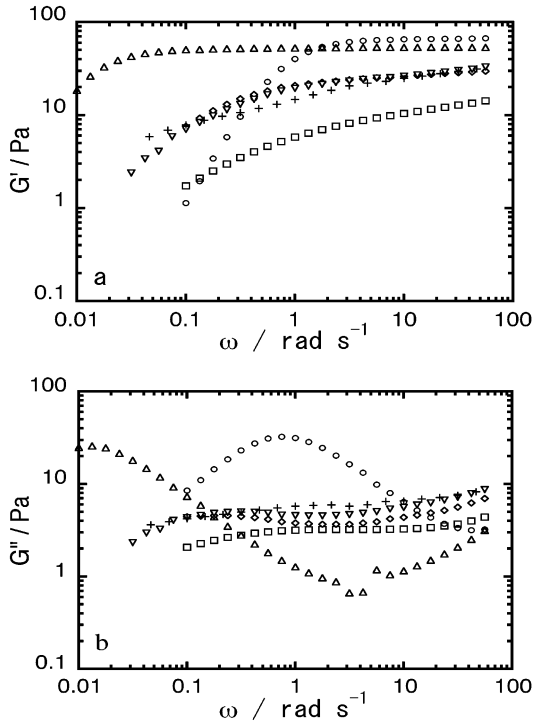

Figure 4. Angular frequency ω dependence of (a) the storage shear modulus G' and (b) the loss shear modulus G'' of oleylDMAO solutions with different degrees of ionization α at $C = 0.15$ M in water at 25 °C: $\alpha = 0$ (open circles), $\alpha = 0.1$ (open triangles), $\alpha = 0.2$ (open squares), $\alpha = 0.3$ (diamonds), $\alpha = 0.4$ (inverted triangles), and $\alpha = 0.5$ (+).

In the range of $\alpha \geq 0.2$, the frequency dependencies of both G' and G'' are weak and $G' > G''$. The shear rate dependence of the solution viscosity at $C = 0.15$ M is shown in Figure 5. All solutions showed shear thinning and the onset shear rates $(d\gamma/dt)^*$ for the shear thinning decreased with increasing α: they were 0.4−0.6, 0.13−0.15, 0.07−0.1, and 0.02−0.04 s^{-1} for $\alpha = 0$, 0.1, 0.2, and 0.3−0.4, respectively. This might be interpreted in terms of possible micelle growth with α, though the amount of micelles is expected to decrease with α as a result of the transformation into vesicles. The viscosity of the solution containing both fibrous micelles and vesicles is expected to be mainly determined by the micelles. At $\alpha = 0.5$, a small yield stress, smaller than 1 Pa, was suggested since we observed that air bubbles could not escape from the solution. These results are consistent with the picture of densely packed particles. Nevertheless, the solution shows shear thinning suggesting a significant contribution from coexisting fibrous micelles.

3. Micelle−Vesicle Conversion in Water at 25 °C and $C = 0.05$ M. The dynamic viscoelastic measurements at 0.05 M were reported previously.[48] At $\alpha = 0$, the Maxwell behavior was still observed at this concentration and the relaxation time τ was about 1.2 s. The relaxation time was thus independent of C just as in the case of C14DMAO micelles.[39] A value of about 7 Pa was found for G'_N, which is about 1/10 of the value at $C = 0.15$ M and is consistent with a relation $G'_N \sim C^{2-2.3}$. At $\alpha = 0.1$, the Maxwell behavior was not well developed, contrary to the case at $C = 0.15$ M. An enhanced flow tendency is clearly seen in Figure 5b for the range of $\alpha \geq 0.2$ as in the case of $C = 0.15$ M.

CryoTEM pictures of the solutions in water showed an entangled network of long fibrous micelles at $\alpha = 0$ and vesicles at $\alpha = 0.5$ as previously reported[22] (parts b and c of Figure 3 in ref 22 should be interchanged). Most vesicles are not perforated at $C = 0.05$ M. The cryoTEM observations on the solutions of intermediate α values of 0.2 and 0.3 are presented in the present study. As shown in Figure 6, neither fused networks of micelles nor vesicles were observed at these two α values. Instead, a network of very long entangled micelles with few branching points is seen at $\alpha = 0.3$. The latter aspect is clearly seen in the upper part of the figure, where the film is very thin and separated micellar threads can be followed over the whole width of the micrograph. At $\alpha = 0.2$, the micelles are shorter than those at $\alpha = 0.3$ and 0 (not shown).

4. Reversibility and Time Courses of the Micelle−Vesicle Conversion in Water. The results described in the preceding sections were obtained with solutions prepared by dissolving solid samples of the prescribed α values. The solutions are expected to correspond to "equilibrium".[22] Solutions of $\alpha = 0.5$ were also prepared from the solutions of $\alpha = 0$ by addition of HCl. The time course of dynamic viscoelastic properties of the solutions at $C = 0.05$ M is shown in Figure 7. The Maxwell-type behavior disappeared within 8 h. Nearly identical results as from solutions prepared by dissolving solid samples were observed at 13 and 25 h after the addition of HCl, as shown in Figure 7a. Thus, as judged from the shear modulus, 13 h turned out to be sufficient for threadlike micelles to transform into vesicles.

The flow property showed an interesting behavior as shown in Figure 7b. The viscosity continued to decrease with time and at 25 h after the addition of HCl it became lower than the final level. Then, the final level of the viscosity was attained after 14 days. At $C = 0.15$ M, both dynamic elasticity (G' and G'') and viscosities coincided fairly well with the equilibrium values after 14 days (not shown).

When the solution of $\alpha = 0.5$ was brought to $\alpha = 0$ by the addition of NaOH, the final level was attained within 8 h with respect to both dynamic viscoelasticity and flow viscosity at $C = 0.05$ M as shown in Figure 8. At $C = 0.15$ M, on the other hand, the Maxwell-type behavior was recovered but complete quantitative agreement was not attained even after 3 weeks, probably because of different ionic strengths due to the production of NaCl during the neutralization process.

5. Comparison of Micelle−Vesicle Conversions in Water and in 0.01 M NaCl. To monitor the change of the viscoelastic property accompanying the micelle−vesicle conversion, values of G' at $\omega = 10$ rad s^{-1} and the zero shear viscosity η_0 are plotted in Figure 9 as functions of the degree of ionization α. Since the plateau modulus G_N was not observed for nonentangled micelle solutions and vesicle dispersions, the G' values are tentatively taken as a relative measure of the elasticity to cover the solutions of different types of aggregates encountered in the present study. At $C = 0.05$ M in water, η_0 could not be determined for α greater than 0.1 and the maximum apparent viscosities are plotted in Figure 9 only to complete the α dependence of the viscosity. For the results obtained in water, minima of both G' and η_0 occur at $\alpha = 0.2$ in the case of $C = 0.15$ M. The low viscoelastic properties of the solution at $\alpha = 0.2$ is consistent with cryoTEM pictures given in Figure 6, which shows the micelles to be shorter at $\alpha = 0.2$ than at $\alpha = 0.3$. Correspondingly, the degree of counterion binding in the range of $\alpha = 0.2-0.28$ shows a slight but significant downward deviation from a theoretical curve, which well describes the results in the remaining range of α.[57] At $\alpha = 0.5$, we observed perforated and normal (nonperforated) bilayer structures (vesicles and lamellae) at $C = 0.15$ and 0.05 M, respectively,[22] and fibrous micelles coexisted with vesicles in the case of $C = 0.05$ M.

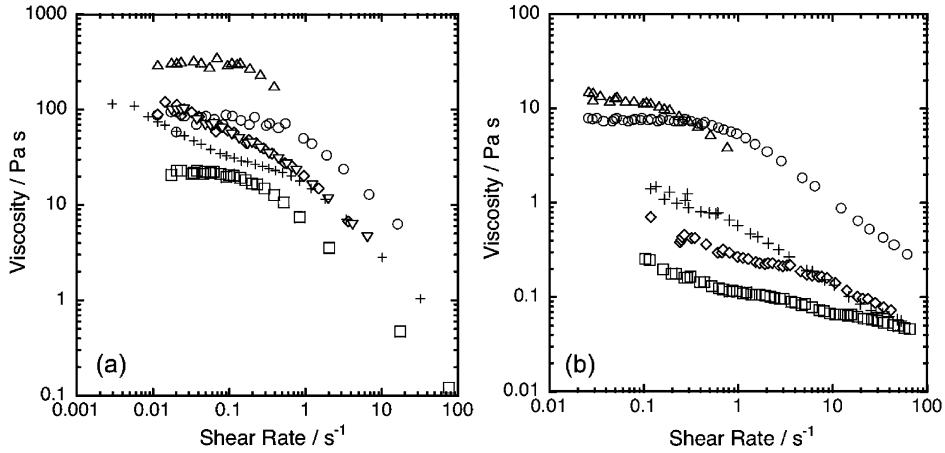

Figure 5. Shear rate dependence of the solution viscosity at different α values at (a) $C = 0.15$ M and (b) $C = 0.05$ M in water at 25 °C: $\alpha = 0$ (open circles), $\alpha = 0.1$ (open triangles), $\alpha = 0.2$ (open squares), $\alpha = 0.3$ (diamonds), $\alpha = 0.4$ (inverted triangles), and $\alpha = 0.5$ (+).

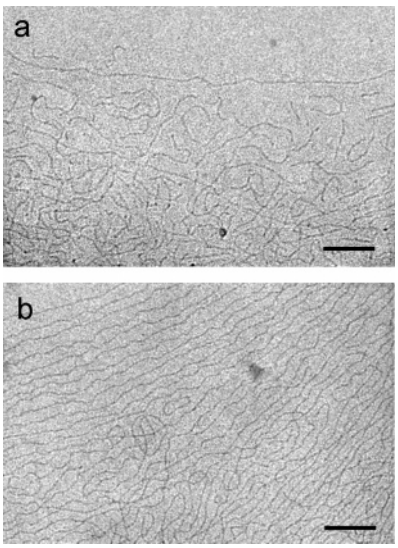

Figure 6. Cryoscopic transmission electron micrographs of oleylDMAO solution at $C = 0.05$ M in water: (a) $\alpha = 0.2$ and (b) $\alpha = 0.3$. The bar in each figure corresponds to 100 nm.

For the results obtained in 0.01 M NaCl at $C = 0.05$ M, minima of G' and η_0 both occur at $\alpha = 0.3$, instead of $\alpha = 0.2$ in water. In 0.01 M NaCl, the lowest viscoelasity at $\alpha = 0.3$ arises from the unique aggregation state, a fused network, clearly shown in Figure 3a. This characteristic structure was not observed in water at either $C = 0.15$ or 0.05 M, although the counterion concentration C_g at $\alpha = 0.3$ is 0.045 M for $C = 0.15$ M in water, which is higher than 0.025 M for $C = 0.05$M in 0.01 M NaCl. Hence, the ratio C_g/C and not only C_g itself seems to be an important factor dictating the aggregate structures of the surfactant in the present study.

Discussion

1. Sequences of Aggregate Structures as Functions of the Degree of Ionization α. Sequences of aggregate structures observed in the present study are summarized in Table 1 as functions of α. In this table "micelles" refer to long fibrous micelles and the data on the counterion binding refer to the surfactant concentration of 0.05 M and are taken from ref 57. In the media of high or medium ionic strengths, the average curvature of amine oxides has been shown to decrease monotonically with increasing α up to $\alpha = 0.5$, both experimentally on dodecyl- and tetradecyldimethylamine oxides[20,39] and theoretically.[58] This characteristic behavior of amine oxides has been ascribed to the hydrogen bonding between the nonprotonated and the protonated headgroups. Generally, charge repulsion makes curvatures larger while in the present system the hydrogen bonding assisted by ionization (protonation) makes curvatures smaller unless the electric repulsion among the hydrogen bonded dimers surpasses the effect. In the present study, we can assume the decreasing curvatures with increasing α in the case of 0.01 M NaCl. The sequence of aggregate structures in 0.01 M NaCl is mostly consistent with the conclusion given in the paper by Porte et al.[51] In water, however, curvatures may increase with increasing α in a range somewhere between 0.2 and 0.3. For simplicity, we assume, except for a region close to $\alpha = 0.5$, that the aggregates are regarded as a two-component mixture of nonionic monomers and the hydrogen bonded (half-protonated) dimers.

In the first stage ($\alpha \leq 0.1$ in water and $\alpha \leq 0.2$ in 0.01 M NaCl) where only micelles are present, average curvatures decrease with increasing α and this leads to the micelle growth. The micelle growth with increasing charge amount is opposite to the observations on many ionic micelles. In the second stage where α increases further, the average curvature continues to decrease in 0.01 M NaCl while in water it is expected to increase in the range of α around 0.2−0.28 where electric repulsion surpasses the hydrogen bond effect. In the third stage where the average curvature becomes smaller beyond that of cylindrical structures, aggregate structures other than fibrous micelles become stable and three options will be considered here: (1) branching of fibrous micelles, (2) "phase separation" into two kinds of aggregates of different curvatures, and (3) formation of (perforated) bilayers.

(1) A molecular theory of branching of cylindrical micelles has been presented.[59] However, a discussion on a macroscopic level would be sufficient in the present context. In fused networks, the junction portions are characterized by negative Gaussian curvatures. As is well-recognized, the junction will be favored when the elastic modulus of the Gaussian curvature k_G is positive according to eq 1. On theoretical grounds, values of k_G of charged membranes are expected to be negative but become less negative as the ionic strength of the medium increases.[8,13−15] In 0.01 M NaCl, a fused network of fibrous micelles appears in this stage. In water, on the other hand, it is expected that k_G is negative enough to exclude negative Gaussian curvatures. (2) In case that negative curvatures are

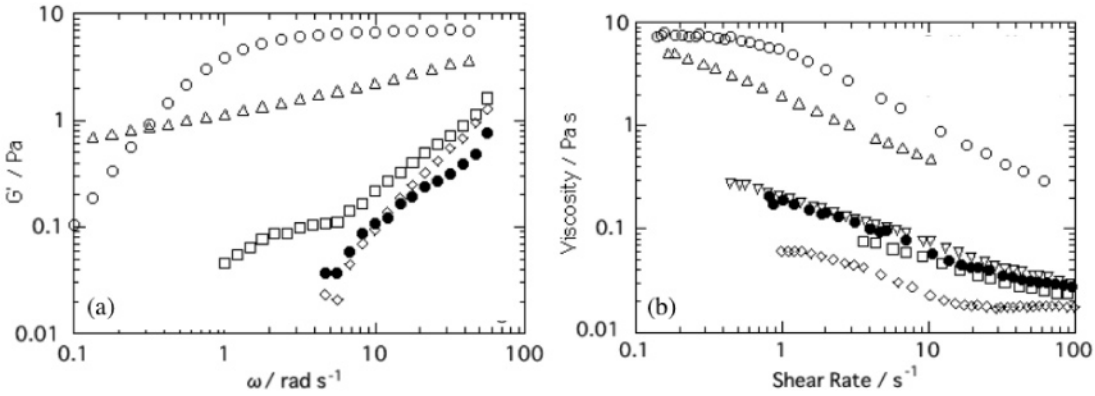

Figure 7. Time course of (a) the storage shear modulus G' and (b) flow viscosity of the solutions at $C = 0.05$ M when the solution of $\alpha = 0$ was brought to $\alpha = 0.5$ by the addition of HCl. Filled circles in parts a and b represent the results obtained with the solutions prepared by dissolving the solid sample of $\alpha = 0.5$. Open circles represent the results at $\alpha = 0$. Time after the addition of HCl: 8 h (triangles), 13 h (squares), 25 h (diamonds), and 14 days (inverted triangels).

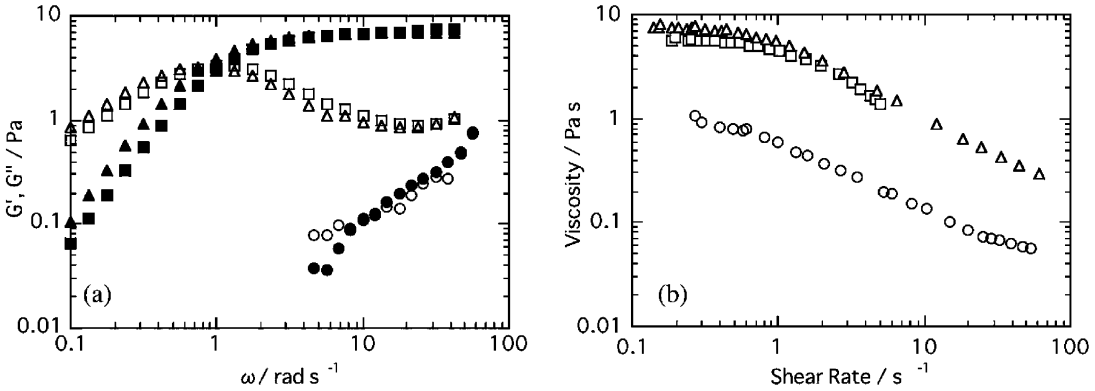

Figure 8. Time course of (a) the storage shear moduli G' (filled symbols) and G'' (open symbols) and (b) flow viscosity of the solutions at $C = 0.05$ M. Squares represent the results on the solution of $\alpha = 0$ observed at 8 h after the addition of NaOH to the solution of $\alpha = 0.5$. Circles and triangles represent the results obtained with the solutions prepared by dissolving the solid sample of $\alpha = 0.5$ and 0, respectively.

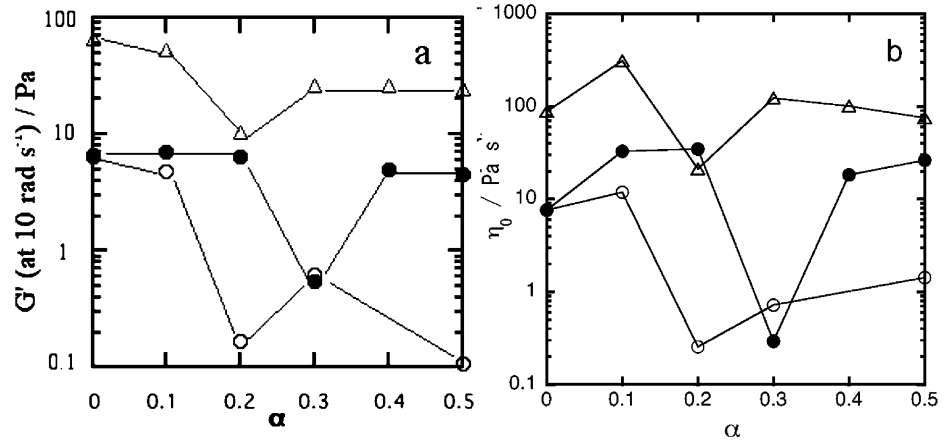

Figure 9. Effects of α on (a) G' ($\omega = 10$ rad s^{-1}) and (b) zero shear viscosities η_0. Filled circles refer to the results in 0.01 M NaCl at $C = 0.05$ M. Open triangles and circles refer to the results in water at $C = 0.15$ and 0.05 M, respectively.

unavailable, a kind of phase separation into two kinds of aggregates of different curvatures may lead to a state of low free energy.[60] This situation has been observed on mixtures of single chain surfactants with double chain lipids.[61,62] We interpret this situation prevails in water in the range $0.4 < \alpha \sim 0.5$: coexistence of fibrous micelles and vesicles. The solution would be regarded as consisting of at least two phases.

According to option 3, we expected that the fused network at $\alpha = 0.3$ in 0.01 M NaCl transformed into perforated vesicles as α increased to 0.4. However, this is not the case and we find instead the "phase separation" into micelles + vesicles. The "phase separation" state is thus suggested to be more stable than either perforated vesicles or a fused network at $\alpha = 0.4$. In the final stage in 0.01 M NaCl, $\alpha = 0.5$, we have found a state of perforated bilayer structures (vesicles + lamellae) that is expected to appear in the Porte scheme next to the state of a fused network with the decreasing average curvature.

2. Thermodynamic/Kinetic Stability of the Vesicles. It is controversial as to whether the stability of amphiphile vesicles is thermodynamic or kinetic.[12,63] In many systems it is obvious that the vesicles are not thermodynamically stable; they are kinetically trapped and best regarded as a dispersion of the

TABLE 1: Micelle−Vesicle Conversion of Oletldimethylamine oxide at 25 °C

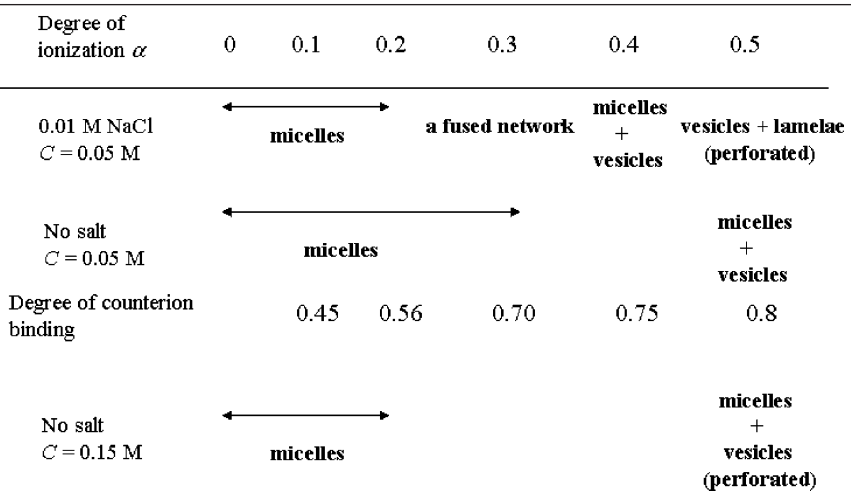

lamellar phase in water or in L_1 phase. Four criteria were recently proposed to be satisfied by vesicles in thermodynamic equilibrium.[64] These are (i) spontaneous formation, (ii) long-time stability with respect to average size and polydispersity, (iii) reversibility with respect to formation and destruction, and (iv) L_1(micelle) and L_α(lamella) phases should be adjacent in the phase diagram. It seems to us that a single criterion could be enough: The vesicle size distribution of particular solution in a given thermodynamic state should be independent of the path of its formation. It was recently shown that spontaneusly formed vesicles in CTAB−sodium octyl sulfate mixtures did not live up to this criterion.[65]

We now examine if our vesicles satisfy these criteria. As to criterion i, vesicles were prepared by the addition of a small aliquot of HCl aqueous solution followed by gentle stirring. It is thus likely they were formed spontaneously, though an effect of the gentle stirring[66] is not excluded. Reversibility with respect to the formation and destruction of the vesicles is satisfied as presented in section 3 but we have not investigated whether the vesicle size distribution remains the same. For oleylDMAO in water, L_1(micelle) and L_α(lamella) phases are adjacent in the phase diagram at $\alpha = 0.5$.[42] In this way, the vesicles in the present study satisfy criteria i, iii, and iv. However, we have not shown that the long-time stability, criterion ii, is fulfilled, and we have not proven the uniqueness of the vesicle size distribution. The question of thermodynamic equilibrium is not settled. Also, a question whether a vesicle suspension consists of a single phase is another issue that has not been solved so far.

3. Synergism between the Nonprotonated and the Protonated Headgroups of Amine Oxides. The synergism between the nonprotonated (nonionic) and the protonated (cationic) headgroups of amine oxides has been observed in several solution properties such as the cmc,[20] aggregation number,[38] and viscoelasticity[39] in the media of moderately high ionic strengths and monolayer structures at a solution/solid interface.[43] The hydrogen bond between the nonionic and the cationic headgroups is considered to be responsible for the synergism. On the other hand, the cmc of dodecyldimethylamine oxide (C12DMAO) in water increases in a monotonic way with increasing α and hence does not show a synergism.[67]

Strong electric repulsion in the media of low ionic strengths surpasses the stabilization of the hydrogen bond. In the present study on oleylDMAO, however, the synergism was observed not only in 0.01 M NaCl solutions but also in water. It is likely that increased attraction between the long alkyl chain of oleylDMAO compensates electric repulsion, which dominates in the case of C12DMAO in water. The synergism in the present study manifests itself as the micelle-to-vesicle transition with increasing charge amount of the system. This is in contrast with the catanionic mixtures where vesicles have smaller net charges than micelles.[25−27]

Conclusions

Reversible micelle-to-vesicle conversion of oleyldimethylamine oxides with increase of the degree of ionization α was confirmed both in water and in 0.01 M NaCl. The conversion is due to the synergism between the protonated and the nonprotonated headgroups of amine oxide. This is in contrast with the case of dodecyldimethylamine oxide on which the synergism has been too weak to be detected in water. The micelle−vesicle conversion was well-detected by viscoelastic properties. Characteristic features of the present system are as follows. (1) The fused network is stable in 0.01 M NaCl but not stable in water. (2) With decreasing average curvature in 0.01 M NaCl, a fused network at $\alpha = 0.3$ transforms into a mixture consisting of fibrous micelles and perforated vesicles at $\alpha = 0.4$ and then finally into perforated vesicles at $\alpha = 0.5$. (3) Bilayers tend to be perforated as the ionic strength of the medium increases.

References and Notes

(1) Engberts, J. B. F. N.; Kevelam, J. *Curr. Opin. Colloid Interface Sci.* **1996**, *1*, 779.
(2) Khan, A.; Marques, E. F. *Curr. Opin. Colloid Interface Sci.* **2000**, *4*, 402.
(3) Lasic, D. D.; Joannic, R.; Keller, B. C.; Frederik, P. M.; Auvray, L. *Adv. Colloid Interface Sci.* **2001**, *89−90*, 337.
(4) Tondre, C.; Caillet, C. *Adv. Colloid Interface Sci.* **2001**, *93*, 115.
(5) Svenson, S. *Curr. Opin. Colloid Interface Sci.* **2004**, *9*, 201.
(6) Gradzielski, M. *Curr. Opin. Colloid Interface Sci.* **2003**, *8*, 337.
(7) Helfrich, W. *Z. Naturforsch.* **1973**, *28C*, 693
(8) Helfrich, W. *Prog. Colloid Polym. Sci.* **1994**, *95*, 7.
(9) Nagarajan, R.; Ruckenstein, E. *J. Colloid Interface Sci.* **1979**, *71*, 580.
(10) Mitchel, D. J.; Ninham, B. W. *J. Chem. Soc., Faraday Trans. 2* **1981**, *77*, 601
(11) Yuet, P. K.; Blankschtein, D. *Langmuir* **1996**, *12*, 3802
(12) Jung, H. T.; Coldren, B.; Zasadzinski, J. A.; Iampietro, D. J.; Kaler, E. W. *Proc. Natl. Acad. Sci. U.S.A.* **2001**, *98*, 1353−1357.
(13) Mitchell, D. J.; Ninham, B. W. *Langmuir* **1989**, *5*, 1121.
(14) Lekkerkerker, H. N. W. *Phys. A* **1989**, *159*, 319.
(15) Winterhalter, M.; Helfrich, W. *J. Phys. Chem.* **1992**, *96*, 327.
(16) Gebicki, J. M.; Hicks, M. *Nature* **1973**, *243*, 232.

(17) Hargrieves, W. R.; Deamer, D. W. *Biochemistry* **1978**, *17*, 3759.
(18) Edwards, K.; Silvander, M.; Karlsson, G. *Langmuir* **1995**, *11*, 2429.
(19) Blochiner, F.; Blocher, M.; Walde, P.; Luisi, P. L. *J. Phys. Chem. B* **1998**, *102*, 10283.
(20) Maeda, H.; Kakehashi, R. *Adv. Colloid Interface Sci*. **2000**, *88*, 275.
(21) Kawasaki, H.; Maeda, H. *Langmuir* **2001**, *17*, 2278.
(22) Kawasaki, H.; Souda, M.; Tanaka, S.; Nemoto, N.; Karlsson, G.; Almgren, M.; Maeda, H. *J. Phys. Chem. B* **2002**, *106*, 1524.
(23) Herve, P.; Rouex, A. M.; Bellocq, A. M.; Nallet, F.; GulikKrzywicki, T. *J. Phys. II* **1993**, *3*, 1225
(24) Gustafsson, J.; Orädd, G.; Nyden, M.; Hansson, P.; Almgren, M. *Langmuir* **1998**, *14*, 4987.
(25) Kaler, E. W.; Murthy, A. K.; Rodriguez, B. E.; Zasadzinski, J. A. *Science* **1989**, *245*, 1371.
(26) Kaler, E. W.; Herrington, K. L.; Murthy, A. K.; Zasadzinski, J. A. N. *J. Phys. Chem.* **1992**, *96*, 6698.
(27) Yatcilla, M. T.; Herrington, K. L.; Brasher, L. L.; Kaler, E. W.; Chiruvolu, S. *J. Phys. Chem.* **1996**, *100*, 5874.
(28) Horbaschek, K.; Hoffmann, H.; Hao, J. *J. Phys. Chem. B* **2000**, *104*, 2781.
(29) Hao, J.; Hoffmann, H.; Horbaschek, K. *J. Phys. Chem. B* **2000**, *104*, 10144.
(30) Hassan, P. A.; Narayanan, J.; Menon, S. V. G.; Salkar, R. A.; Samant, S. D.; Manohar. C. *Colloid Surf. A* **1996**, *117*, 89.
(31) Narayanan, J.; Manohar, C.; Kern, F.; Candau, S. J. *Langmuir* **1997**, *13*, 5235.
(32) Kawasaki, H.; Miyahara, M.; Almgren, M.; Karlsson, G.; Maeda, H. *J. Colloid Interface Sci.* **2005**, *284*, 349.
(33) Yin, H. Q.; Huang, J. B.; Zhang, Y. Y.; Qiu, S. C.; Ye, J. P. *J. Phys. Chem. B* **2005**, *109*, 4104.
(34) Johnsson, M.; Wagenaar, A.; Engberts, J. B. F. N. *J. Am. Chem. Soc.* **2003**, 125, 757.
(35) Gonzalez, Y. I.; Nakanishi, H.; Stjerndahl, M.; Kaler, E. W. *J. Phys. Chem. B* **2005**, *109*, 11675.
(36) Rydhag, L.; Stenius, P.; Ödberg, L. *J. Colloid Interface Sci*. **1982**, *86*, 274.
(37) Lasic, D. D. *J. Liopsome Res.* **1999**, *9*, 43.
(38) Kaimoto, H.; Shoho, K.; Sasaki, S.; Maeda H. *J. Phys. Chem.* **1994**, *98*, 10243.
(39) Maeda, H.; Yamamoto, A.; Kawasaki, H.; Souda, M.; Hossain, K. S.; Nemoto, N.; Almgren, M. *J. Phys. Chem. B* **2001**, *105*, 5411
(40) Kawasaki, H.; Syuto, M.; Maeda, H. *Langmuir* **2001**, *17*, 8210.
(41) Miyahara, M.; Kawasaki, H.; Imahayashi, R.; Maeda, H. *Prog. Colloid Polym. Sci,*. **2004**, *129*, 62.
(42) Kawasaki, H.; Sasaki, A.; Kawashima, T.; Sasaki, S.; Kakehashi, R.; Yamashita, I.; Fukada, K.; Kato, T.; Maeda H. *Langmuir* **2005**, *21*, 5731.
(43) Kawasaki, H.; Shinoda, M.; Miyahara, M.; Maeda, H. *Colloid Polym. Sci.* **2005**, *283*, 359
(44) Hoffmann, H.; Kalus J.; Thurn, H.; Ibel, K. *Ber. Busenges. Phys. Chem.* **1983**, *87*, 1120.
(45) Cates, M. E. *Macromolecules* **1987**, *20*, 2289.
(46) Shikata, T.; Hirata, H.; Kotaka, T. *Langmuir* **1987**, *3*, 1081.
(47) Hoffmann, H.; Thunig, C.; Schmiedel, P.; Munkert, U. *Langmuir* **1994**, *10*, 3972.
(48) Miyahara, M.; Kawasaki, H.; Garamus, V. M.; Nemoto, N.; Kakehashi, R.; Tanaka, S.; Annaka, M.; Maeda, H. *Colloids Surf. B* **2004**, *38*, 131.
(49) Hofmann, S.; Hofmann, H. *J. Phys. Chem. B* **1998**, *102*, 5614.
(50) Mendes, E.; Narayanan, J.; Oda, R.; Kern, F.; Candau, S. J.; Manohar, C. *J. Phys. Chem. B* **1997**, *101*, 2256.
(51) Porte, G.; Gomati, R.; El Hataimy, O. J.; Appel, J.; Marignan, J. *J. Phys. Chem.* **1986**, *90*, 5746.
(52) Appel, J.; Porte, G.; Khatory A.; Kern, F.; Candau, S. J. *J. Phys.* (*France*) *II* **1992**, *2*, 1045.
(53) Danino, D.; Talmon, Y.; Levy, H.; Beinert, G.; Zana, R. *Science* **1995**, *269*, 1420.
(54) Lin, Z. *Langmuir* **1996**, *12*, 1729.
(55) Gustafsson, J.; Orädd, G.; Lindblom, G.; M.; Olson, U.; Almgren, M. *Langmuir* **1997**, *13*, 852.
(56) Khatory, A.; Kern, F.; Lequeux, F.; Apell, J.; Porte, G.; Morie, N.; Ott, A.; Urbach, W. *Langmuir* **1993**, *9*, 933.
(57) Ono, Y.; Kawasaki, H.; Annaka, M.; Maeda, H. *J. Colloid Interface Sci*. **2005**, *287*, 685.
(58) Terada, Y.; Maeda, H.; Odagaki. T. *J. Phys. Chem. B* **1997**, *101*, 5784.
(59) May, S.; Bohbot, Y.; Ben-Shaul, A. *J. Phys. Chem. B* **1997**, *101*, 8648.
(60) Andelman, D.; Kozlov, M. M.; Helfrich, W. *Europhys. Lett*. **1994**, *25*, 231.
(61) Ollivon, M.; Eidelman, O.; Blumenthal, R.; Walter, A. *Biochemistry* **1988**, 27, 1695.
(62) Gustafsson, J.; Orädd, G.; Almgren, M. *Langmuir* **1997**, 13, 6956.
(63) Laughlin, R. G. *Colloids Surf. A* **1997**, *128*, 27.
(64) Marques, E. F. *Langmuir* **2000**, *16*, 4798.
(65) Almgren, M.; Rangelov, S. *Langmuir* **2004**, *20*, 6611.
(66) Bergmeier, M.; Hoffmann, H.; Thunig, C. *J. Phys. Chem. B* **1997**, *101*, 5767.
(67) Imaishi, Y.; Kakehashi, R.; Nezu, T.; Maeda, H. *J. Colloid Interface Sci*. **1998**, *197*, 309.